Supporting Information

Ducret et al. 10.1073/pnas.1120979109

SI Materials and Methods

Bacterial Strains, Plasmids, and Growth. Primers, plasmids and their mode of construction are listed in Tables S2 and S3. See also Table S4 for strains. *Myxococcus xanthus* strains were grown at 32 °C in CYE rich media as previously described (1). Plasmids were introduced in *M. xanthus* by electroporation. Mutants and transformants were obtained by homologous recombination on the basis of a previously reported method. The Wza^0 was obtained after deletion of all of the putative Wza-like exopolysaccharides/capsular polysaccharides EPS/CPS translocons (as determined by Blast analysis and previous literature) (2–4) encoded by the MXAN1915, *fdgA* (MXAN3225) (5, 6) and *epsY* (MXAN7417) (7) genes. Loss of EPS export at the surface of the Wza^0 mutant was tested in the calcofluor white (CFW) EPS detection assay: cells (10 μL), at a concentration of 4×10^9 cfu mL^{-1}, were spotted onto CYE plates containing 1.5% (15 g/L) agar and 5 mg/mL CFW. The plates were incubated at 32 °C for 72 h and photographed with an Olympus SZ61 binocular under exposure to UV lights, as previously described (7) (Fig. S3*B*).

Keratinocyte Cell Line and Growth. Normal human epidermal keratinocytes (NHEK CC-2501; Lonza) were cultured at 37 °C in keratinocyte basal medium (KBM) (Lonza) modified with supplements and growth factors (CC 4456 KGM-CD; Lonza). After 1 wk of culture, they are seeded in microscopy cells with a fibronectin-treated wet-surf at the bottom and imaged by wet-surface–enhanced ellipsometric contrast (Wet-SEEC) 1 or 2 d later.

Carbonyl Cyanine-M-Chlorophenylhydrazone (CCCP) Injections. CCCP-injection experiments were performed as previously described (8) on an A-motile *ΔpilA* strain to ascertain that the drugs specifically affected gliding motility. Briefly, the injection experiments were conducted in a microfluidic chamber where cells were immobilized on a chitosan-treated surface. CCCP injections (10 μM) in TPM medium were performed by a coupled computerized injector system at a flow rate of 1 μL/s. To ensure that CCCP did not kill the cells, CCCP effect reversibility was checked by flushing the microfluidic chamber with TPM.

Lectin Staining Procedure. ConcanavalinA (ConA)-conjugated FITC (ConA-FITC; Sigma-Aldrich) and other lectins (Table S1) (Vector Laboratories) were dissolved in distillated water to give a 2-mg/mL stock solution. Immediately before the experiments, the lectins were diluted in TPM containing 100 mM of $CaCl_2$ and 100 μg/mL of bovine serum albumin (BSA). The mixture was then injected into the flow chamber. After 20 min of incubation, the lectins were washed out with TPM containing 100 mM of $CaCl_2$ and 100 μg/mL of BSA.

Surface Coating for Cell Immobilization. The cell immobilization procedure was performed as previously described (8). Briefly, channels were filled with 1 mL of agarose DMSO (Sigma-Aldrich) solution (0.75% wt/vol). Ten minutes later channels were washed with 1 mL distilled water, and 1 mL of the overnight cell culture was injected into the tunnel. After 30 min, floating cells were flushed out with 1 mL of TPM.

Time-Lapse Video Microscopy. Time-lapse experiments were performed as previously described (9). Microscopic analysis was performed using an automated and inverted epifluorescence microscope TE2000-E-PFS (Nikon). The microscope is equipped with the Perfect Focus System (PFS) that automatically maintains focus so that the point of interest within a specimen is always kept in sharp focus at all times, despite any mechanical or thermal perturbations. Images were recorded with a CoolSNAP HQ 2 (Roper Scientific) and a 40×/0.75 DLL Plan-Apochromat or a 100×/1.4 DLL objective. All fluorescence images were acquired with appropriate filters with minimal exposure time to minimize bleaching and phototoxicity effects. Cell tracking was performed automatically using a previously described macro under the METAMORPH software (Molecular Devices), when appropriate, manual measurements were also performed to correct tracking errors with tools built into the software (9). Typically, the images were equalized, straightened, and overlaid under both ImageJ 1.40g (National Institutes of Health) and METAMORPH.

SI Text S1

To further test slime secretion by nonmotile cells, we used CCCP, a component that collapses the proton motive force and blocks the motility motors (9, 10). Upon exposure to CCCP, the cells stopped moving immediately, an effect that was rapidly reversed when CCCP was washed from the microfluidic chamber (Fig. S3*C*). As expected, slime deposition was significantly enriched at the area where the cells had stopped, blocked by the CCCP treatment (Fig. S3*C*).

SI Text S2

On the chitosan substrate, gliding cells often detach, presumably due to the shear stress in the microfluidic chamber (Fig. S5*B*). We found that detachment from the substrate is correlated to cell velocity so that faster moving cells were more likely to detach than slower moving cells (Fig. S5*A*). Knowing that cells deposit less slime when they move faster, this suggests that slime promotes adhesion to the chitosan substrate. In addition, cells sometimes detach partially and remain attached by a cell pole. This adhesion cannot result from polar pili because the bacterial strain used for these experiments lacks *pilA*, the gene encoding the main pilus subunit. In fact, in all these cases, the cell poles remained attached to large patches of slime (Fig. S5*B*), further suggesting that slime promotes adhesion.

1. Bustamante VH, Martínez-Flores I, Vlamakis HC, Zusman DR (2004) Analysis of the Frz signal transduction system of Myxococcus xanthus shows the importance of the conserved C-terminal region of the cytoplasmic chemoreceptor FrzCD in sensing signals. *Mol Microbiol* 53:1501–1513.
2. Dong C, et al. (2006) Wza the translocon for E. coli capsular polysaccharides defines a new class of membrane protein. *Nature* 444:226–229.
3. Beis K, et al. (2004) Three-dimensional structure of Wza, the protein required for translocation of group 1 capsular polysaccharide across the outer membrane of Escherichia coli. *J Biol Chem* 279:28227–28232.
4. Drummelsmith J, Whitfield C (2000) Translocation of group 1 capsular polysaccharide to the surface of Escherichia coli requires a multimeric complex in the outer membrane. *EMBO J* 19:57–66.
5. Müller F-D, Treuner-Lange A, Heider J, Huntley SM, Higgs PI (2010) Global transcriptome analysis of spore formation in Myxococcus xanthus reveals a locus necessary for cell differentiation. *BMC Genomics* 11:264.
6. Ueki T, Inouye S (2005) Identification of a gene involved in polysaccharide export as a transcription target of FruA, an essential factor for Myxococcus xanthus development. *J Biol Chem* 280:32279–32284.
7. Lu A, et al. (2005) Exopolysaccharide biosynthesis genes required for social motility in Myxococcus xanthus. *Mol Microbiol* 55:206–220.
8. Sun M, Wartel M, Cascales E, Shaevitz JW, Mignot T (2011) Motor-driven intracellular transport powers bacterial gliding motility. *Proc Natl Acad Sci USA* 108:7559–7564.
9. Ducret A, et al. (2009) A microscope automated fluidic system to study bacterial processes in real time. *PLoS ONE* 4:e7282.
10. Nan B, et al. (2011) Myxobacteria gliding motility requires cytoskeleton rotation powered by proton motive force. *Proc Natl Acad Sci USA* 108:2498–2503.

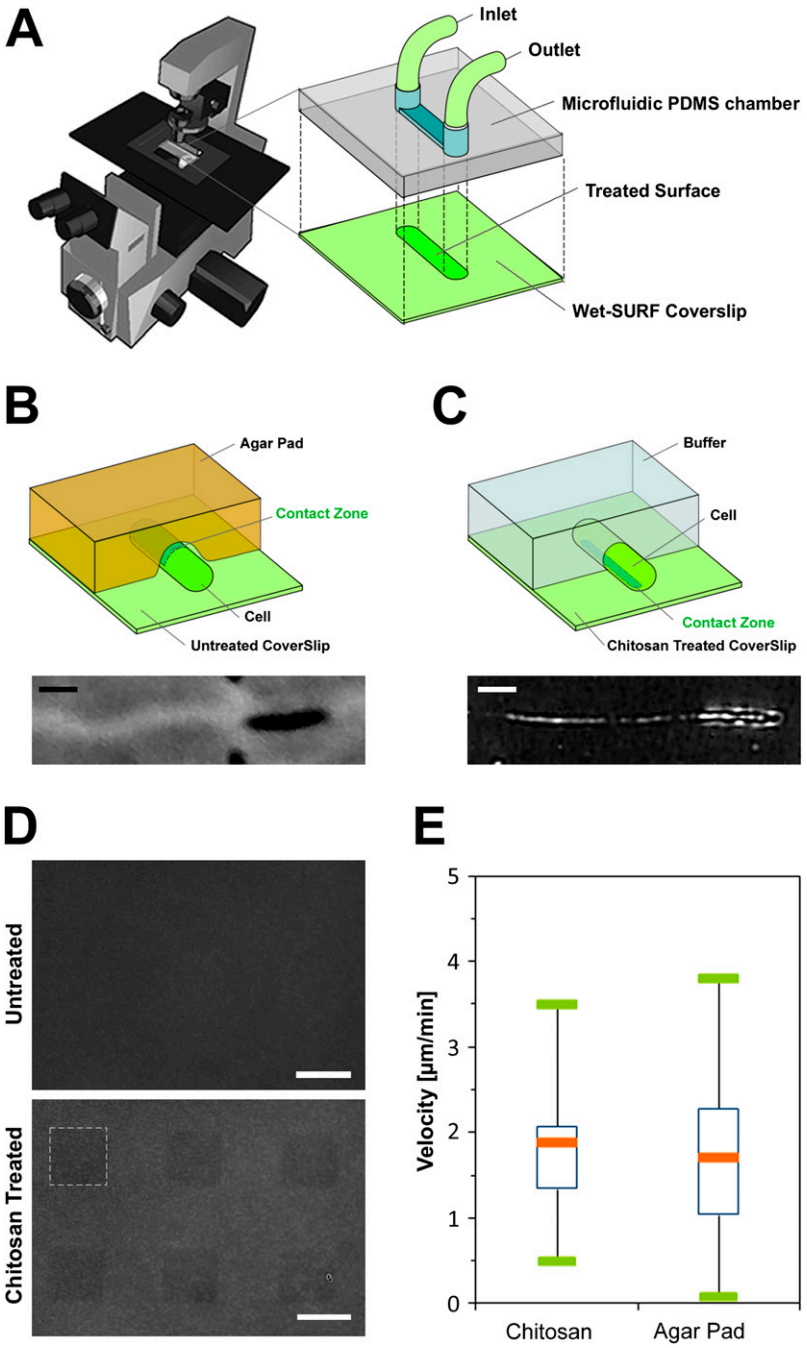

Fig. S1. Motility of *Myxococcus* cells on chitosan-treated wet-surf. (*A*) Schematics of the Wet-SEEC setup. A chitosan-treated wet-surf coverslip is placed directly on the stage of a standard inverted microscope. A microfluidic polydimethylsiloxane (PDMS) chamber is mounted on the wet-surf in our experiments. (*B*) Schematic representation of a standard agar pad system and a resulting phase contrast image of a slime trail. In this system, the cell body is in contact with the substrate (dark green area) through its upper face (relative to the coverslip) and the relatively low hardness of the substrate presumably allows extended contact points around the cell cylinder. (Scale bar, 1 μm.) (*C*) Schematic representation of the chitosan-treated wet-surf and resulting Wet-SEEC image of a slime trail. In this system, the cell establishes contacts directly on the coverslip and, due to the hardness of glass, the contact zone is limited to the area that intersects between the cell cylinder and the coverslip plane (dark green area). (Scale bar, 1 μm.) (*D*) Wet-SEEC images of untreated and chitosan-treated wet-surfs. Chitosan was deposited by micropatterning (*Materials and Methods*). Dark square zones (pointed by a white square in dashed line) represent untreated surface areas, whereas brighter zones represent the chitosan-treated surface. (Scale bar, 10 μm.) (*E*) Motility of *Myxococcus* cells on chitosan versus agar. Box plots of the average velocity of 100 cells are shown.

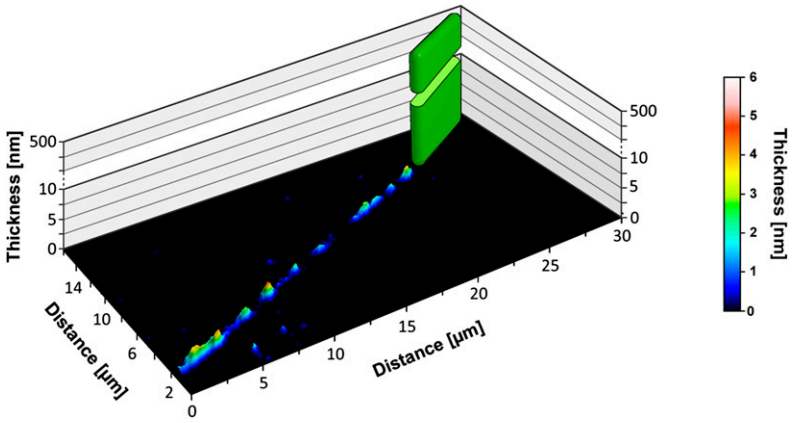

Fig. S2. Topographic 3D reconstruction of the slime trail. Cell body is schematically representated in green.

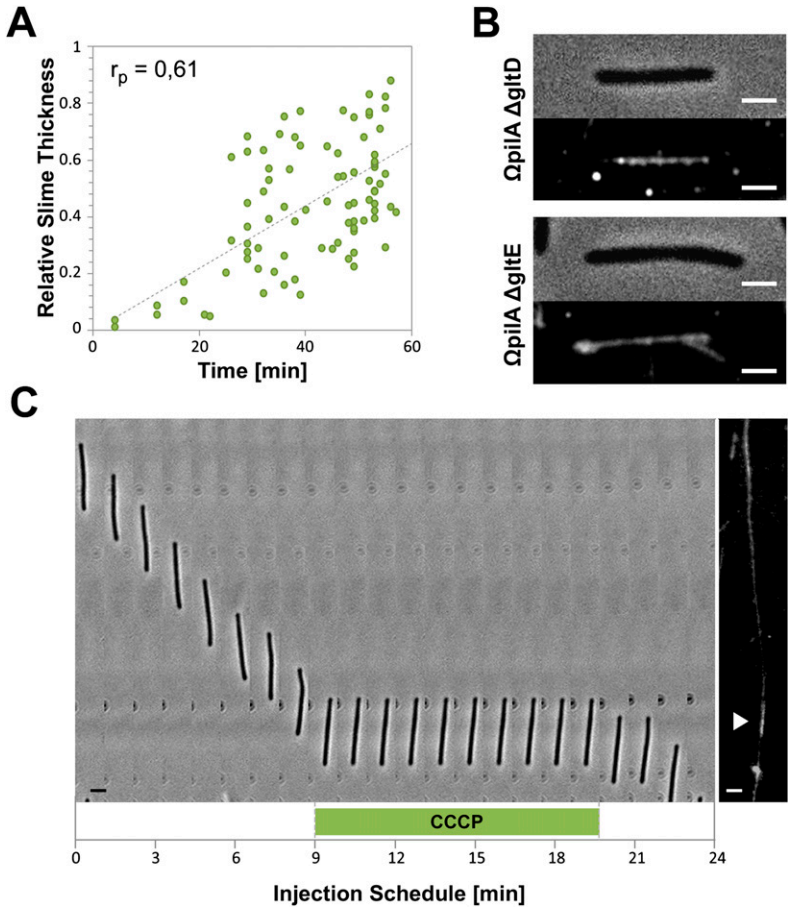

Fig. S3. Slime is deposited at constant rates underneath the cell body of nonmotile or immobilized cells. Cells were allowed to settle on the substratum and flushed at different times. (*A*) Relative slime thickness (as measured by Wet-SEEC) is plotted against flushing time for 100 cells (Rp, Pearson coefficient). (*B*) Ω*PilA* Δ*GltD* and Ω*PilA* Δ*GltE* mutant cells were allowed to settle on the substratum and flushed after 60 min of incubation. Slime deposition underneath the cell body was observed using Wet-SEEC. (Scale bar, 1 μm.) (*C*) Cell movements before, during, and after CCCP injection are shown by phase contrast. The corresponding Wet-SEEC slime trail is significantly thicker (white triangle) at locations where the cell stopped, blocked by the CCCP treatment. (Scale bar, 1 μm.)

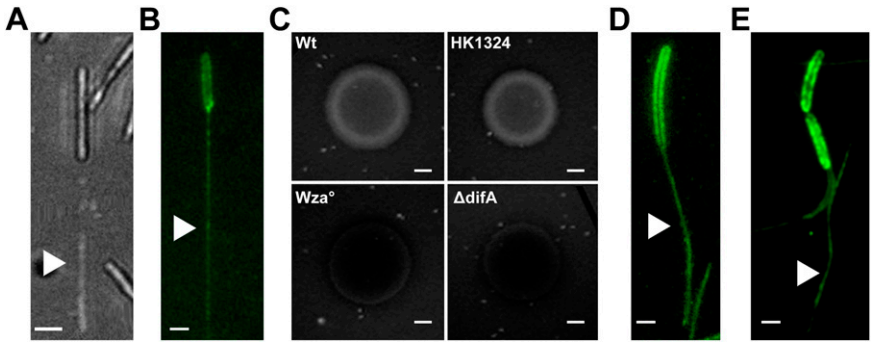

Fig. S4. Slime is still deposited by EPS and O-antigen defective strains. (*A*) Wet-SEEC images of slime deposition in the wake of a *wza*° mutant cell. (Scale bar, 1 μm.) (*B*) ConA-staining image of slime deposition in wake of a *wza*° mutant cell. (Scale bar, 1 μm.) (*C*) Calcofluor white binding of *M. xanthus* colonies, as described in *SI Materials and Methods*. Binding of calcofluor white to EPS results in a fluorescent ring seen in wild type (WT) or sasA mutant (HK1324). The *wza*° and *difA* mutants do not bind the calcofluor white dye. (Scale bar, 5 mm.) (*D*) ConA-staining image of slime deposition in wake of a LPS-O-antigen mutant cell (HK1324). (Scale bar, 1 μm.) (*E*) ConA-staining image of slime deposition in wake of *difA* mutant cells. (Scale bar, 1 μm.)

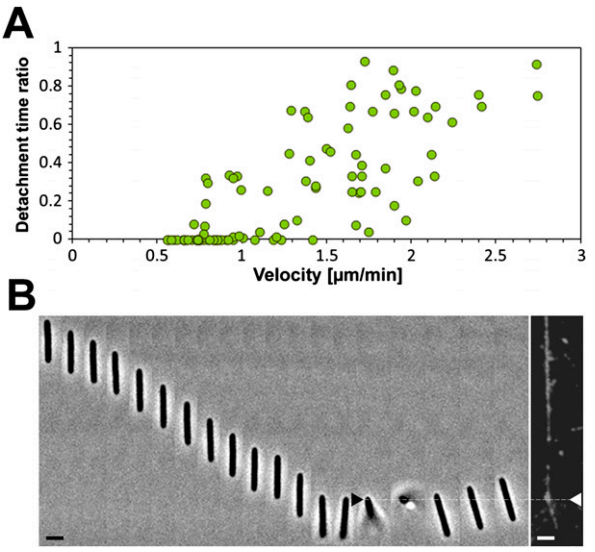

Fig. S5. Slime mediates adhesion. (*A*) Correlation between cell substrate attachment and cell velocity for 100 cells. Detachment time ratio is the ratio of the amount of time spent by a given cell on the substrate over the total time of the experiment (120 min). (*B*) Flipping cell and its associated slime trail. Dotted line shows the point of cell pole attachment, which correlates with a significantly slime-enriched area (white triangle). (Scale bar, 1 μm.)

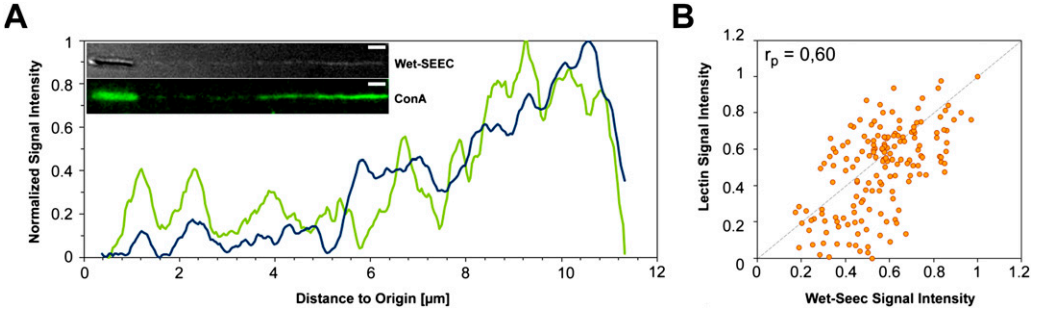

Fig. S6. Slime trails observed on Wet-SEEC images are mainly composed of polysaccharides. (*A*) Comparison of the slime trail profiles observed by Wet-SEEC image (blue line) and after ConA staining (green line). Both images used for analysis are shown in the *Inset*. (Scale bar, 1 μm.) (*B*) Correspondence between the relative amounts of slime measured by Wet-SEEC and ConA staining (Rp, Pearson coefficient).

Table S1. Lectins used in this study and their respective staining pattern (cell body and slime trails)

Lectin	Source	Cell body	Slime trails
ConA	*Canavalia ensiformis*	++++	++++
LCH/LCA	*Lens culinaris*	—	—
GNA	*Galanthus nivalis*	—	—
PSA	*Pisum sativum* (garden pea) seeds	—	—
RCA	*Ricinus communis*	—	—
PNA	*Arachis hypogaea*	—	—
VVL/VVA	*Vicia villosa*	—	—
ECL	*Erythrina cristagalli* seeds	—	—
Jacalin	*Artocarpus integrifolia* (jackfruit) seeds	—	—
DBA	*Dolichos biflorus* (horse gram) seeds	—	—
SBA	*Glycine max* (soybean) seeds	—	—
WGA	*Triticum vulgaris*	+	—
GSL	*Griffonia (Bandeiraea) simplicifolia*	—	—
DSL	*Datura stramonium* (thorn apple or Jimson weed) seeds	—	—
LEL/TL	*Lycopersicon esculentum* (tomato)	—	—
STL	*Solanum tuberosum* (potato)	—	—
MAL	*Maackia amurensis*	—	—
UEA	*Ulex europaeus*	—	—

Table S2. Primers used in this study

Primer name	Sequences of primers (5′–3′)
1915–1	CCCAAGCTTCCGTCGTCCACGCTG
1915–2	GAAGAAGCTCTCCGGGCGGAAGCTGGTCATCTCCA
1915–3	ATGACCAGCTTCCGCCCGGAGAGCTTCTTCTAGCC
1915–4	CGGGATCCAAGGTGCGGGGCATG
3225–1	GCTCTAGACAGGTCCACCGGCTGC
3225–2	CGACGACGGTGTCACCCGGCCGCGCGCTCGTCTTGCCCAT
3225–3	ATGGGCAAGACGAGCGCGCGGCCGGGTGACACCGTCGTCGTTCCG
3225–4	CGGGATCCTGGGTGAAACGGCGCG
7417–1	GCTCTAGAGGTGCCGCTGGTGGCG
7417–2	CCACGTCACCGGGGCGCATGAGCGGTGGAACTCTCC
7417–3	CACCGCTCATGCGCCCCGGTGACGTGGTGGTGGTGGAATAAC
7417–4	CGGGATCCTCCGTGAAGGGGACGA

Table S3. Plasmids used in this study

Plasmid name	Construction scheme
pBJ114	Used to create deletions, galK, KmR (Laboratory collection).
pBJΔ1915	Primer pairs 1915–1/1915–2 and 1915–3/1915–4 were used to amplify 1-kb fragments upstream and downstream from the MXAN_1915 open-reading frame. Overlap fragment were obtain by overlapping PCR with the upstream and the downstream fragment as matrice. Then, overlap fragment was ligated at the BamHI and HindIII sites of the pBJ114.
pBJΔfdgA	Primer pairs 3225–1/3225–2 and 3225–3/3225–4 were used to amplify 1-kb fragments upstream and downstream from the MXAN_3225 open-reading frame. Overlap fragment were obtain by overlapping PCR with the upstream and the downstream fragment as matrice. Then, overlap fragment was ligated at the BamHI and XbaI sites of the pBJ114.
pBJΔepsY	Primer pairs 7417–1 /7417–2 and 7417–3 /7417–4 were used to amplify 1-kb fragments upstream and downstream from the MXAN_7417 open-reading frame. Overlap fragment were obtain by overlapping PCR with the upstream and the downstream fragment as matrice. Then, overlap fragment was ligated at the BamHI and XbaI sites of the pBJ114.

Table S4. Strains used in this study

Strain	Description	Source	Genotype
DZ2	Wild type	Laboratory collection	WT
TM156	DZ2 *pilA::tet*	Laboratory collection	*ΩpilA*
TM389	DZ2 ΔpilA	Laboratory collection	*ΔpilA*
TM1	DZ2 ΔdifA	Laboratory collection	ΔdifA
TM146	DZ2 ΔaglQ	(1)	*ΔaglQ*
TM449	DZ2 ΔpilAΔaglQ	(1)	*ΔpilAΔaglQ*
TM453	DZ2 ΔpilAΔaglQmx8att::aglQmCherry	(1)	*ΔpilAΔaglQaglQ-mCherry*
TM340	DZ2 ΔaglQmx8att::aglQmCherryaglZ-YFP	(1)	*ΔaglQaglQ-mCherryaglZ-YFP*
TM253	DZ2 *pilA::tet* ΔgltD	(2)	*ΩpilA ΔgltD*
TM297	DZ2 *pilA::tet* ΔgltE	(2)	*ΩpilA ΔgltE*
TM529	DZ2 Δ1915	This work	*Δ1915*
TM484	DZ2 ΔfdgA	This work	*ΔfdgA*
TM469	DZ2 ΔepsY	This work	*ΔepsY*
TM530	DZ2 Δ1915 ΔfdgA ΔepsY	This work	*Wza°*
HK1324	DK1622 Ωwzt wzm wbgA	(3)	*ΩsasA*

1. Sun M, Wartel M, Cascales E, Shaevitz JW, Mignot T (2011) Motor-driven intracellular transport powers bacterial gliding motility. *Proc Natl Acad Sci USA* 108:7559–7564.
2. Luciano J, et al. (2011) Emergence and modular evolution of a novel motility machinery in bacteria. *PLoS Genet* 7, 10.1371/journal.pgen.1002268.
3. Bowden MG, Kaplan HB (1998) The Myxococcus xanthus lipopolysaccharide O-antigen is required for social motility and multicellular development. *Mol Microbiol* 30:275–284.

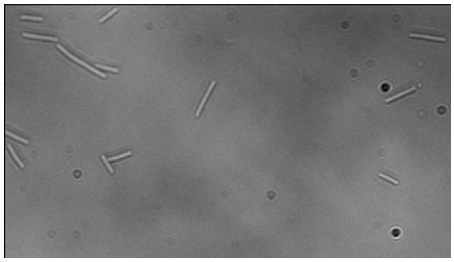

Movie S1. Live observation of *Myxococcus* cells moving on the chitosan-treated surface. Phase contrast images of motile cells (*ΩPilA* mutant cells) shown at different time points. Pictures were taken every 30 s. (Scale bar, 1 μm.)

Movie S1

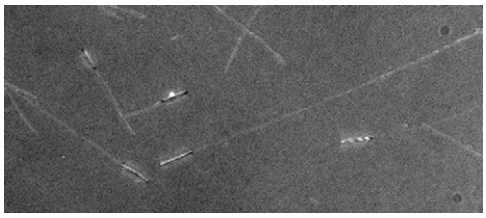

Movie S2. Live observation of *Myxococcus* slime trails deposition as images by Wet-SEEC. Wet-SEEC images of slime deposition in the wake of motile cells (*ΩPilA* mutant cells) shown at different time points. Pictures were taken every 30 s. (Scale bar, 1 μm.)

Movie S2

Movie S3. Topographic 3D reconstruction of a slime trail. The green mass represents the cell.

Movie S3

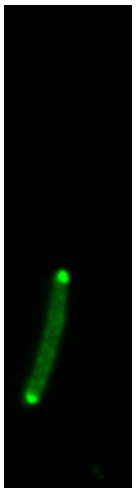

Movie S4. Slime is deposited by the motility complexes during motility. ConA-staining images of a moving cell (*ΩPilA* mutant cells) and resulting slime trail at different time point. Pictures were taken every 30 s. For details, see Fig. 4*A*.

Movie S4

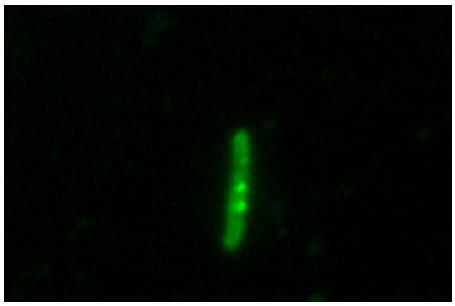

Movie S5. ConA clusters are transported down the cell body in immobile cells (*ΩPilA* mutant cells). Pictures were taken every 15 s. For details, see Fig. 4*B*.

Movie S5